R004-01
Zoom meeting A ：11/4 AM1 (9:00-10:30)
9:00〜9:15

Near-seafloor magnetic anomaly reveals geomagnetic field fluctuation during 29?33 Myr

#Masakazu Fujii[1,2)],Kyoko Okino[3)],Chiori Tamura[3)]
([1]NIPR,[2]SOKENDAI,[3]AORI, Univ. Tokyo

Knowledge of the Earth's magnetic field intensity variations has been obtained through a record of archaeomagnetic and volcanic materials, and sedimentary sequences. Although geomagnetic field intensity signal recorded as the oceanic crust should provide higher and longer time-resolution continuous record (e.g., Gee et al., 2000), available data is essentially limited due to observation difficulty. Here, we present new observation data of near-seafloor magnetic anomalies of 29-33 Myr seafloor at the Southeast Indian Ridge. We conducted a deep-tow operation during the R/V Hakuho-maru cruise of KH-20-1. Deep-sea total magnetic fields were measured using the deep-tow cesium magnetometer developed by AORI, The University of Tokyo. The sensor reached ˜4,500m deep. The total length of obtained data at $>$3,000m deep is up to 40 miles. Collected near-seafloor magnetic anomaly ranges 60,700 to 62,300 nT, which provides variation three times larger than the total intensity variation simultaneously observed at sea-surface. Long-wavelength signatures are well correlated with each other. Considering continuous surface magnetic data from 0-age ridge axis and geomagnetic polarity chrons (e.g., Gee and Kent, 2015), we individually picked magnetic isochrons of C11n12n, C11r, C12n, and C12r from obtained near-seafloor magnetic anomalies. Several tiny wiggles with an amplitude of up to 300 nT are remarkably observed in C12r. This result is generally consistent with summarized cryptochrons (Cande and Kent, 1992; Cande and Kent, 1995). A few tiny wiggles with an amplitude of up to 200 nT were also observed in C12n, which have never been reported in magnetic anomaly data. This variation is well correlated with records from sediment of Pacific equatorial zone (Yamazaki et al., 2013; Yamamoto et al., 2013), and lava flow of the Lima Limo section of the Ethiopian trap (Ahn et al., 2021; Yoshimura et al., 2020). Our results clearly demonstrate that southern Indian oceanic crust well recorded paleo-geomagnetic field intensity during early Oligocene concurrently with Ethiopian lava and Pacific sediment.

R004-02
Zoom meeting A ：11/4 AM1 (9:00-10:30)
9:15〜9:30

Magnetic and gravity constraints on crustal structure of the Nosappu Fracture Zone, Northwestern Pacific

#Mai Kintsu[1)],Masakazu Fujii[2,3)],Tomoko Hanyu[4)],Nobukazu Seama[1)]
([1]Dept. of Planetology, Kobe Univ.,[2]NIPR,[3]SOKENDAI（The Graduate University for Advanced Studies),[4]KOBEC

Fracture zones are linear oceanic features that extend past the transform faults, away from the mid-ocean ridge axis. They are distinct from transform faults, but they have features associated with transform faults and show evidence of past activity. Understanding the structure and lithology of fracture zones provides insight into the long-term behavior of oceanic crust, such as magnetic field variations, crustal accretion processes, and temporal change of lithology. The bathymetry, magnetic anomaly and gravity anomaly data around the Nosappu Fracture Zone located on the old Pacific lithosphere were acquired during two research cruises; the KR06-03 with R/V Kairei and YK14-09 with R/V Yokosuka. Multiple analyses of these data sets were carried out for an interpretation of features of the NFZ together with the adjacent oceanic crusts, and a suggestion of constraints on the crustal structure and relationship with their tectonic background.

To estimate paleo-inclination and declination of oceanic crust, reduction to the pole (RTP) processing of magnetic anomalies was conducted. The paleo magnetization direction was determined by comparing obtained topographic features with the RTP anomaly. After that, equivalent magnetization was estimated from magnetic anomaly based on the well-established inversion methods (e.g., Macdonald et al., 1980; Parker & Huestis, 1974), assuming a 1.0 km thick magnetized source layer and magnetization without vertical variation. In addition, mantle Bouguer anomaly (MBA) was calculated from the satellite-derived free-air gravity anomaly (Sandwell et al., 2014) and newly collected multibeam bathymetry data using the method of Parker (1973).

The obtained bathymetric data shows steep valley walls of the NFZ, and abyssal hills in the oceanic crust to the west of NFZ and J-shaped ridges in the oceanic crust to the east of NFZ. The low intensity of the crustal magnetization is observed along the NFZ area. In the oceanic crust to the east of NFZ, observed characteristic features of magnetization, with the slightly curved to the north along the western edge, are similar to the features of bathymetric J-shape ridge. Anomalous negative MBA also appears around the NFZ area, suggesting the exposure of high-density material or thin crustal thickness.

The results of these analyses provide the basis of the magnetization structure model. Based on the parameters determined by the RTP operation, we interpret that the oceanic crust around the NFZ was formed and magnetized in the southern hemisphere. This interpretation is generally consistent with the global plate reconstruction model of Seton et al.(2012). By combining the results of analyses, It could be mentioned that the magnetization structure of the eastern oceanic crust adjacent to the NFZ retains the crustal structure from the time of the transform-fracture zone system.

R004-03
Zoom meeting A ：11/4 AM1 (9:00-10:30)
9:30〜9:45

Energy transfer among the equatorially symmetric components of magnetic and flow fields during dipole reversals in geodynamo model

#Takumi Kera[1)],Hiroaki Matsui[2)],Masaki Matsushima[3)],Yuto Katoh[1)]
([1]Dept. Geophys., Grad. Sch. Sci., Tohoku Univ.,([2]UC Davis,([3]Tokyo Tech

Paleomagnetic observations have revealed that the geomagnetic field has reversed its polarity a number of times. Numerical dynamo simulations have represented dipole reversals and provided insights into physical processes that give rise to the polarity reversals. Both paleomagnetic observations and numerical dynamos have inferred that the equatorial symmetry of the magnetic and velocity fields is related to polarity reversals. The tilt of the virtual geomagnetic dipole obtained by the paleomagnetic field observations during the past 150 Ma shows that geomagnetic field reversed polarity more frequently when the geomagnetic field was more symmetrical with respect to the equator (McFadden et al., 1991). Dynamo simulations revealed a strong inverse correlation between the stability and the equatorial symmetry of the magnetic field (Coe and Glatzmaier, 2006). Olson et al., (2004) proposed a process of magnetic polarity reversals in a dynamo model. In their model, the reversed magnetic field flux is produced locally in the convective plumes near the inner core boundary and transported from one hemisphere to the other hemisphere by the meridional circulation. This result suggests that anti-symmetric flow with respect to the equator plays a large role in reversals. This anti-symmetric flow is enhanced when the magnetic dipole is reversed. Nishikawa and Kusano (2008) explained this asymmetric velocity field enhancement by enhancement of energy transfer from magnetic field to asymmetric velocity field in polarity reversal phase by the Lorentz force. However, Nishikawa and Kusano (2008) set large magnetic Prandtl number (Pm=15), and there is no comparison of contribution between the amplitude of the Lorentz force and buoyancy. In the present research, we investigate how anti-symmetric flow is growing and maintained in the dynamo in which reversals occur with lower Pm.

We perform dynamo simulations using Calypso (Matsui et al., 2014) to represent dipole dominant dynamo with reversals. In the present study, we set the fixed heat flux, non-slip, and connecting the potential field at the inner and outer boundaries as the boundary conditions for temperature, velocity, and magnetic field, respectively. For the dimensionless numbers, we set dimensionless numbers to Ekman number E = 6x10^{-4}, Prandtl number Pr = 1, magnetic Prandtl number Pm = 5 and modified Rayleigh number Ra = 2000. We investigate the energy fluxes in terms of the symmetricity with respect to the equator in the stable polarity phase and in the polarity reversal phase, respectively.

When the dipole magnetic field sustains stably, the symmetric component is dominant for the velocity field, and magnetic field is dominated by the anti-symmetric components. On the other hand, during the reversal, flow fields are nearly anti-symmetric outside the tangent cylinder, while symmetrical and anti-symmetrical magnetic fields are comparable in amplitude. The energy conversion between components of different symmetry is also analysed.

We decompose the buoyancy fluxes for the symmetric and antisymmetric flow as $<$Ra T_s $\mathbf{u}_s$. $\mathbf{r}/r_o>$and $<$Ra T_a $\mathbf{u}_a$. $\mathbf{r}/r_o>$where subscripts s and a indicates symmetric and anti-symmetric components, respectively. We also decompose work of Lorentz force $<\mathbf{u}_s$. ($\mathbf{J}_s$ $\hat{}\mathbf{B}_a)>$, $<\mathbf{u}_s$. ($\mathbf{J}_a$ $\hat{}\mathbf{B}_s)>$, $<\mathbf{u}_a$. ($\mathbf{J}_s$ $\hat{}\mathbf{B}_s)>$and $<\mathbf{u}_a$. ($\mathbf{J}_a$ $\hat{}\mathbf{B}_a)>$. In the reversal phase, buoyancy flux to asymmetric velocity field $<$Ra T_a $\mathbf{u}_a$. $\mathbf{r}/r_o>$increases 1.05 times of that in the stable phase, while $<$Ra T_s $\mathbf{u}_s$. $\mathbf{r}/r_o>$decrease 0.98 times of that in the stable phase. This result may explain that asymmetric velocity field is enhanced in the reversal phase. Looking at the work of Lorentz force in the stable polarity phase, energy transfer from the symmetric velocity to the symmetric magnetic field -$<\mathbf{u}_s$. ($\mathbf{J}_a$ $\hat{}\mathbf{B}_s)>$keeps 0.92 times of the symmetric velocity to the antisymmetric magnetic field -$<\mathbf{u}_s$. ($\mathbf{J}_s$ $\hat{}\mathbf{B}_a)>$. In the reversal phase, only the energy transfer from the symmetric flow to antisymmetric magnetic field decreases from the stable dipolar phase, resulting that -$<\mathbf{u}_s$. ($\mathbf{J}_a$ $\hat{}\mathbf{B}_s)>$is 1.12 times larger than -$<\mathbf{u}_s$. ($\mathbf{J}_s$ $\hat{}\mathbf{B}_a)>$. This change can make the amplitude of the symmetric component of the magnetic field comparable to that of the anti-symmetric component during the reversal. In addition, conversion of asymmetric velocity to asymmetric magnetic field $<\mathbf{u}_a$. ($\mathbf{J}_s$ $\hat{}\mathbf{B}_s)>$remains up to 90% of that in the stable phase, while the other terms decrease to nearly 60% from the stable phase. Consequently, asymmetric velocity field more contribute to generate antisymmetric magnetic field than in stable phase.

R004-04
Zoom meeting A ：11/4 AM1 (9:00-10:30)
9:45〜10:00

A preliminary study of the Hadean geodynamo based on a Basal-Magma-Ocean-Dynamo hypothesis

#Futoshi Takahashi[1)]
(1)Kyushu Univ.

From Paleomagnetic studies, it is suggested that the geodynamo has been active for ca. 4.2 billion years (Tarduno et al., 2020). During such a long lifetime of the geodynamo it is often argued that the geomagnetic field is maintained without the solid inner core in the Hadean and Archean eons. Moreover, a younger age of the inner core formation is preferred based on high electrical conductivity of the core material (e.g., Ohta et al., 2016). However, there is a debate regarding energy source maintaining thermally-driven convection and also a dynamo for such a long time interval without the inner core. We consider a hypothesis that the early geodynamo was maintained by a dynamo action in the lowermost part of the melted mantle, i.e. Basal Magma Ocean (BMO) dynamo. Thermal history calculations suggest that the BMO dynamo is likely in terms of core energetics (Ziegler and Stegman, 2013), whereas any geodynamo simulations have not yet been carried out. Here we show a result of our pilot study to see whether the BMO could really be a dynamo. In our model, it is assumed that the core is perfectly conducting and the BMO layer is very thick, which should be much thinner compared with the core size in the ancient Earth. Keeping these assumptions in mind, our preliminary survey of the BMO dynamo is reported.

R004-05
Zoom meeting A ：11/4 AM1 (9:00-10:30)
10:00～10:15

伊能忠敬の山島方位記から十九世紀初頭の日本の地磁気偏角を解析する。第10回報告

#辻本 元博[1)]
(1 なし

Analyzing the early 19th century’s geomagnetic declination in Japan from Tadataka Inoh

#Motohiro Tsujimoto[1)]
(1none

The Santou-Houi-Ki is a national treasure of Japan consist of 67 volumes ledger of approximately 200,000 azimuth data by 0 deg 5 min unit in 1800 to 1816 cover from eastern Hokkaido to Yakushima island recorded by cartographic surveyor Tadataka Inoh.

We execute interdisciplinary and simultaneous analysis of real azimuth, magnetic declination, magnetic compass survey azimuth, the target points in latitude and longitude and the survey reference point in latitude and longitude where the value of declination to any targets are similar or proximate.

It is necessary to introduce the geomagnetic declination data analyzed from The Santou-Houi-Ki, to Andrew Jackson’s Gufm1 or NOAA’s Historical Declination Viewer, because the lack of declination data in Japan from mid 17 century to mid 19 century equal to the term of national isolation of Japan.

The analyzed position of survey reference point in latitude and longitude will be further detailed by referring to the old and new maps created by the Geospatial Information Authority of Japan and the old and new maps registered by the Ministry of Justice.

It can be used detailed positions in local history which was impossible with the research methods of the liberal arts of each university.

国宝山島方位記地図測量家伊能忠敬により 1800 年から 1816 年に記録された北海道東部から屋久島迄の 67 巻の磁針測量方位角原簿で測量実施地点の地名と 0 度 05 分単位の推計約 20 万件の磁針測量方位角が記録されている。山島方位記から測量対象地点、測量実施地点の各緯度経度、真方位、地磁気偏角を学際で同時解析をする。測量実施地点位置からいずれの測量対象地点への磁針測量方位角にも含まれる地磁気偏角が一定或いは近似になる位置を逆算解析する。

山島方位記から解析した地磁気偏角を 17 世紀中期から 19 世紀期迄日本の鎖国の為に地磁気偏角データが不足するアンドリュージャクソンの GUFM1 及び NOAA の Historical Declination Viewer に導入する必要がある。

解析された測量実施地点の緯度経度位置は国土地理院の新旧の地図、法務省の新旧登記図により更に詳細になる。従来はどの大学の文系での研究方法では不可能であった郷土史上の詳細地点の研究で活用可能である。

江戸時代の旧東海道白須賀の宿場での測量実施地点の傍の記念石碑はこの解析により研究され設置された最初の石碑である。

R004-06
Zoom meeting A ：11/4 AM2 (10:45-12:30)
10:45～11:15

An improved apparent polar wander path for southwest Japan: Cenozoic multi-phase rotations with respect to the Asian continent

#Koji Uno[1)],Yuta Idehara[1)],Daichi Morita[1)],Kuniyuki Furukawa[2)]
([1]Okayama Univ.,[2]Aichi Univ.

To construct the Mesozoic apparent polar wander path (APWP) for the inner arc of the southwestern Japanese islands (referred to as southwest Japan) and compare it to that of East Asia, a 110 Ma paleomagnetic pole for southwest Japan was determined. Sedimentary rock samples were collected from 16 sites for paleomagnetic analysis in the Lower Cretaceous Inakura Formation in the central part of southwest Japan. A primary remanent magnetization component, with unblocking temperatures of 670-695 C, was isolated from 11 sites. The primary directions combined with the previously reported ones provide a new mean direction (D = 79.7, I = 47.4, a95 = 6.5, N = 17), and a corresponding paleomagnetic pole that is representative of southwest Japan (24.6 N, 203.1 E, A95 = 6.8). The Early Cretaceous paleomagnetic pole, together with the Late Cretaceous and Cenozoic poles, constitute a new APWP for southwest Japan. The new APWP illustrates a standstill polar position during 110-70 Ma, suggesting tectonic quiescence of this region. This standstill was followed by two large tracks during the Cenozoic. We interpret these tracks as clockwise tectonic rotations of southwest Japan that occurred twice during the Cenozoic. The earlier tectonic rotation occurred for a tectonic unit positioned below northeast China, the Liaodong and Korean Peninsulas, and southwest Japan (East Tan-Lu Block) during the Paleogene. The later rotation took place only under southwest Japan during the Neogene. Cenozoic multiphase rifting activity in the eastern margin of the Asian continent was responsible for the tectonic rotations that are observed from the paleomagnetic studies.

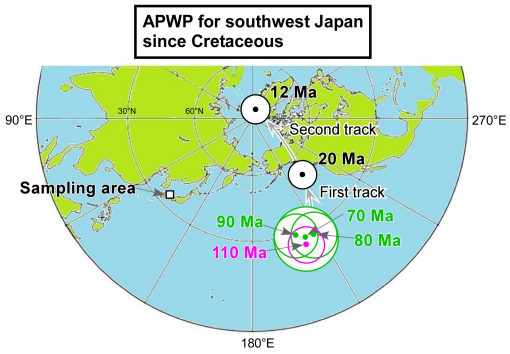

R004-07
Zoom meeting A ：11/4 AM2 (10:45-12:30)
11:15〜11:30

富士火山における紀元前 3600 から 1000 年の古地磁気方位

#馬場 章 [1)], 渋谷 秀敏 [2)]
(1 富士山研,(2 同志社大

Paleomagnetic direction data during 3600 to 1000 BCE at Fuji volcano, Japan

#Akira Baba[1)],Hidetoshi Shibuya[2)]
(1MFRI,Yamanashi Perf.,(2Doshisha Univ.

The paleomagnetic secular variation (PSV) records in Japan has mainly been restored by archaeomagnetic studies of old kilns and hearths (e.g. Hirooka, 1977) and paleomagnetic studies of sediment cores (e.g. Ali et al., 1999). The volcanic materials can also be a very good candidate reconstructing the PSV. We have presented the paleomagnetic direction measurements of the volcanic products on Fuji volcano to draw the PSV curve from CE 1100 to 1000 BCE (Baba and Shibuya, 2020). Here, we try to extend the PSV curve at Fuji volcano beyond 1000 BCE.

Volcanic products before 1000 BCE are widely distributed on the Fuji volcano as lava flows and pyroclasts. Takada et al. (2016) categorized 43 rock-stratigraphic units with the ages of 3600 to 1500 BCE into Subashiri-b stage. However, the ^{14}C data are sparse thus eruption ages have been mostly estimated using the tephrostratigraphy by trench excavations of each pyroclastic cone (e.g. Ishizuka et al.,2007). Therefore, we conducted the paleomagnetic study of those volcanic products to fill the gap of the ^{14}C aged units. From each volcanic product, we collected 6 to 20 samples using an engine powered core picker. Samples were oriented by a sun compass to eliminate the influence of local magnetic anomalies. Magnetization of the samples are measured using a spinner magnetometer, and magnetic cleaning is performed with alternating field demagnetization and thermal demagnetization.

Although the magnetic direction dataset is not large enough to draw a credible PSV curve before 1000 BCE, most of the paleomagnetic directions before 1000 BCE shows the easterly declination, and agree with the known the PSV curve drawn at Aso volcano. Correlating the volcanic materials in two volcanoes by the paleomagnetic direction, we may resolve the ^{14}C age scarcity problem.

R004-08
Zoom meeting A ：11/4 AM2 (10:45-12:30)
11:30〜11:45

復元窯試料を用いた考古地磁気強度実験の妥当性の検討:その２

#北原 優[1)], 畠山 唯達[1)], 山本 裕二[2)]
[1)] 岡山理大・フロンティア,[2)] 高知大

Examination of the validity of the archaeointensity experiment using the samples from reconstructed pottery kiln : Part 2

#Yu Kitahara[1)],Tadahiro Hatakeyama[1)],Yuhji Yamamoto[2)]
[1)]Frontier Science and Technology, Okayama Univ. Sci,[2)]Kochi University

The reconstruction of secular variation of archaeointensity has been an important research theme in archaeomagnetism in recent years. In Japan, an archaeointensity dataset and a secular variation reference curve were constructed in 2021 using the latest experimental methods (the Tsunakawa-Shaw method and the IZZI-Thellier method). The intensity data obtained after the 2000s, including this Japanese dataset, is much more reliable than datasets reported before the 2000s, because these were reconstructed using the latest experimental methods and data selection criteria. However, there is still some dispersion in the data (the coefficient of variation ranges from single-digit percentages to percentages over 10 and less than 20), and it is observed that the dispersion is not homogeneous and clusters into a plurality of intensity values, especially in some sites.

Considering the cause of the variation, and in order to further improve the accuracy of the estimation of archaeointensity, we carried out archaeointensity experiments by the Tsunakawa-Shaw method using the baked earth samples and pottery fragment samples collected from the reconstructed ancient pottery kiln, and observe the dispersion in the obtained intensity data. As experimental samples, we used the kiln floor (black in color), kiln wall (black and red in color), and product (gray in color) taken from the kiln (Bizen City, Okayama Prefecture) reconstructed by Tadashi Hirakawa, a ceramic artist of Bizen ware. As a result of the experiment, the mean intensities obtained that passed the data selection criteria were 45.8 +/- 2.4 μ T (n=8) from the kiln floor, 48.8 +/- 6.8 μ T (n=8) from the kiln wall, and 46.7 +/- 2.8 μ T (n=3) from the product. Then, it was confirmed that the mean intensities of these three samples correspond to the observed field intensity (47.5 μ T) near the kiln within 1 σ. However, regarding the data of the kiln wall, the coefficient of variation was significantly large compared to the other samples, and it was observed that the data also clustered in the black and red parts of the kiln wall.

In addition, a more detailed archaeointensity experiment was carried out using the kiln wall samples. In this experiment, the kiln wall samples were processed into five pieces of 1.5 cm each in depth, and each specimen was used for the experiment of the Tsunakawa-Shaw method (in vacuum and in air) and the experiment of the IZZI-Thellier method (in air). As a result, in the Tsunakawa-Shaw method, the intensity values (46.4 in vacuum, 46.9 μ T in air) consistent with the observed intensity values were estimated from the specimen at a depth of 1.5-3.0 cm from the surface, while a low intensity value of approximately 10 μ T was estimated from the specimens at 0.0-1.5 cm (including the glass layer of the surface), and a high intensity value of approximately 4-7 μ T was estimated from the specimens at 3.0-7.5 cm (the part with the red color). On the other hand, in the IZZI-Thellier method, the archaeointensity (45.3-50.7 μ T) close to the observed intensity value was estimated from the specimens at 3.0-7.5 cm, while a low intensity value of approximately 8 μ T was estimated from the specimens at 0.0-3.0 cm.

In the future, an experiment of the IZZI-Thellier method in vacuum and microscopic observation for sister samples will also be carried out, and the causes of these intensity dispersions will be considered together with the results of archaeomagnetic experiments.

考古地磁気強度の永年変化の推定は、近年の考古地磁気学における重要な研究テーマのひとつである。日本においても、「綱川－ショー法」と「IZZI －テリエ法」といった最新の実験手法によって推定した考古地磁気強度データセットに基づき、永年変化標準曲線を 2021 年に論文報告している (Kitahara et al., 2021)。これらのデータセットを含む、2000 年代以降に論文等で報告されている強度データは、最新の実験手法やデータ選別基準を用いて推定されたものであるため、信頼性が高い。しかしながら、それでも「同一と見なせる資料内（＝サイト）」においてデータのばらつきは存在し（変動係数：数%〜十数%）、また、形成時期が同時と見なせる異なるサイト間においても、複数の異なる強度値にクラスタ化してしまうこともある。

これらの原因について示唆を得て、今後の考古地磁気強度研究のさらなる高精度化に資するため、現代の焼き物窯から採取した焼土試料や土器片試料を対象に「綱川－ショー法」による考古地磁気強度実験を実施した。具体的には、備前焼作家の平川忠氏が 2018 年に最終焼成した実験窯（岡山県備前市）の窯床（黒色）・窯壁（黒色および赤色）・製品（灰色）からの試料を使用した。データ選別基準に合格した平均強度値と標準偏差値として、窯床から 45.8 ± 2.4 μ T（n=8）、窯壁から 48.8 ± 6.8 μ T（n=8）、製品から 46.7 ± 2.8 μ T（n=3）という結果が得られた。いずれも、実験窯付近での観測磁場値（47.5 μ T）と標準偏差の範囲で一致する。しかしながら、窯壁からのデータ群に関しては変動係数が他の二者に比べて顕著に大きく、窯壁の黒色部分と赤色部分とでそれぞれ異なる強度値に分かれてクラスタ化していることが原因として考えられた。

そこで、窯壁試料を対象に追加実験を実施した。具体的には、窯の内側表面から外側（深さ）方向に向かって 1.5

cm 間隔で 5 つの試片×３列に細断し、それぞれの試片を対象に「綱川－ショー法」実験（真空中および空気中）と「IZZI －テリエ法」実験（空気中）を行った。「綱川－ショー法」では、1.5-3.0 cm 区間の試片から観測値に近い強度値（真空中：46.4 μ T, 空気中 46.9 μ T）が推定された反面、0.0-1.5 cm 区間の（表面のガラス層を含む）試片からは約 10 μ T 程度低めの強度値が推定され、3.0-7.5cm 区間の（赤色の）試片からは 4-7 μ T 程度高めの強度値が推定された。「IZZI －テリエ法」実験では、3.0-7.5 cm 区間の試片からは観測値に近い強度値（45.3-50.7 μ T）が推定された反面、0.0-3.0cm 区間の試片からは約 8 μ T 程度低めの強度値が推定された。

今後は、さらに真空中での「IZZI －テリエ法」実験と、姉妹試料の鏡下観察を実施し、別途得られている岩石磁気実験の結果と併せて、これらの強度の「ずれ」の原因について考察を深めていく予定である。

R004-09
Zoom meeting A ：11/4 AM2 (10:45-12:30)
11:45〜12:00

西之島 2014-2015 年溶岩による古地磁気強度絶対値測定

#山本 裕二[1)], 小田 啓邦[2)], 多田 訓子[3)], 吉本 充宏[4)], 前野 深[5)], 武尾 実[5)]
([1] 高知大,[2] 産総研・地質情報,[3] 海洋研究開発機構 海域地震火山部門,[4] 富士山研,[5] 東大・地震研

Absolute paleointensity measurements on lavas erupted at Nishinoshima volcano during 2014-2015

#Yuhji Yamamoto[1)],Hirokuni Oda[2)],Noriko Tada[3)],Mitsuhiro Yoshimoto[4)],Fukashi Maeno[5)],Minoru Takeo[5)]
([1]Kochi University,[2]IGG, GSJ, AIST,[3]IMG, JAMSTEC,[4]MFRI, Yamanashi Perf.,[5]ERI, Univ. Tokyo

A volcanic rock formed after 1900, when the International Geomagnetic Reference Field (IGRF) has been determined, is useful as a ”natural standard sample” to assess the reliability of the absolute paleointensity (API) estimation method. We report the results of API measurements using the Tsunakawa-Shaw method on lava formed in 2014-2015 on Nishinoshima Island, one of the Izu-Ogasawara Islands, Japan.

国際標準地球磁場モデル (International Geomagnetic Reference Field, IGRF) が決定されている 1900 年以降に形成した火山岩（歴史溶岩）は、古地磁気強度絶対値 (API) 推定法の信頼性を検証するための「天然標準試料」として有用である。今回は、伊豆・小笠原諸島の 1 つである西之島で 2014-2015 年にかけて形成した溶岩を対象として、「綱川・ショー法」による API 測定を行ったので、結果を報告する。

西之島は、元々は 1973-1974 年噴火による溶岩と、さらに古い活動による溶岩からなる小島であった（海野・中野, 2007）。2013 年 11 月初旬に噴火が開始し、2014 年 10 月までには新しい溶岩流によりほぼ旧西之島は覆い尽くされ、この「第 1 期」の活動は 2015 年末まで継続した（前野ほか, 2018）。2016 年 10 月に「西之島火山活動調査と活動監視のための体制の整備」を主題とする、研究船「新青丸」による KS-16-16 次研究航海が実施され、一連の噴火開始以来初となる上陸調査が 10 月 20-21 日にかけて実施された（前野ら, 2017）。西之島西岸からは 10 を越える地点から岩石ブロック試料が採取され、うち 1 地点からは簡易定方位（クリノメーターによる磁北方向と水平線の記録）による岩石ブロック試料も採取された。

今回の研究では、1 地点からの簡易定方位ブロック試料と、7 地点からの発泡度の異なるブロック試料 (Dense, 2 地点; Intermediate, 2 地点, Porous, 3 地点) を測定対象とした。各ブロック試料からは、2-8 本の直径 1 インチのミニコア試料を採取し、さらに約 2 cm 長の試片を整形して自然残留磁化 (NRM) を測定するとともに、「綱川・ショー法」による API 測定に供した。NRM 強度は 4.6〜41.6 A/m であり、平均は 27.0 A/m、標準偏差は 12.1 A/m であった。API 測定の結果は、ブロック試料毎の平均が 35.4〜46.4 μ T と幅がある一方で、ブロック試料内の標準偏差は 0.9〜3.5 μ T と一定程度のまとまりを示した。発泡度による分類で Dense および Intermediate とされたブロック試料内の標準偏差は 0.9〜1.5 μ T と相対的に小さかったが、Porous とされたブロック試料内の標準偏差は 1.8〜2.3 μ T と相対的に大きかった。後者のブロック試料のほうが、岩石磁気的にやや内部不均質が大きいためと思われるが、検証を進めていく必要がある。全ブロック試料の API の平均は 41.3 μ T、標準偏差は 4.4 μ T となり、西之島の位置における 2014-2015 年の IGRF-13 (Alken et al., 2021) によるモデル磁場値の 41.7 μ T を 10 パーセント程度以内の精度で推定できていると結論できる。

R004-10
Zoom meeting A ：11/4 AM2 (10:45-12:30)
12:00〜12:15

Paleointensity dating for submarine volcanic rocks: a case study at Izu Oshima

#Yoichi Usui[1)],Iona McIntosh[1)],Osamu Ishizuka[2)]
([1]JAMSTEC,[2]GSJ/AIST

Dating volcanic rocks provide a foundation for understanding the evolution of volcanoes. Volcanic activity on the order of 1000 years is also important for disaster prediction. However, dating in this range is often difficult for submarine volcanoes, where radiocarbon dating is unavailable. In this talk, we present paleointensity age constraints for recent submarine basalts around Izu Oshima. The samples were collected in 2009 from submarine ridges in the southeast of Izu Oshima Island. Geochemical data are reported in Ishizuka et al. (2014) and are interpreted to reflect activity over the past 20 kyr. Furthermore, correlating with subaerial volcanics with age information, chemical signatures corresponding to the addition of backarc components at ca. 10-5 ka were observed in some samples. However, more detailed ages are currently unknown. Because sample orientations were not recorded, we focused on geomagnetic intensity (paleointensity) using the Tsunakawa-Shaw protocol. Rock magnetic data indicate that the samples generally contain Ti-rich titanomagnetite with the blocking temperature around 350 $^{\circ}$C. The magnetic properties of the sample do not change much when heated in Ar or vacuum. So far, we have estimated the paleomagnetic intensities of three ridges (SE1, SE2, and SE3). SE1 shows a moderate value of about 45 μ T, while the ridges SE2 and SE3 record relatively strong magnetic fields of about 60 μ T. Comparing with the global and local paleointensity data, such a high paleointensity could be correlated to ca. 8-10 ka. Together with the geochemical data, We interpret SE2 and SE3 to be 8-10 ka and SE1 $<$2 ka.These results indicate that paleomagnetism may improve the dating of submarine volcanic rocks.

Ishizuka et al. (2014) JVGR, 285, 1-17. https://doi.org/10.1016/j.jvolgeores.2014.08.006

R004-11
Zoom meeting A ：11/4 PM1 (13:45-15:30)
13:45〜14:00

Optimization of Tsunakawa-Shaw paleointensity measurements for single plagioclase grains

#Chie Kato[1)],Masahiko Sato[2)],Masao Ohno[1)]
([1]Division of Earth Sciences, SCS, Kyushu Univ.,([2]Dept. EPS, UTokyo

Measurements on single silicate grains are sometimes useful to retrieve paleomagnetic records from samples that are not suitable for general whole rock measurements. It is powerful for plutonic rocks in which the magnetic carriers are dominated by coarse-grained particles, and volcanic rocks which are vulnerable to thermal alteration. Depending on the forming condition and history of the rock, plagioclase crystal contain magnetically stable tiny exsolved grains of magnetite and/or magnetically unstable coarse-grained magnetic minerals or do not significantly contain magnetite. Plagioclase is contained in various types of rocks, and plagioclase crystals containing tiny exsolved grains are often used in single-crystal paleomagnetic study. On another front, acicular exsolved magnetite preferentially oriented in relation to the crystal lattice of the host plagioclase may cause large magnetic anisotropy, and the measurement results of paleointensity and direction must be interpreted with care. Therefore, to efficiently obtain reliable paleomagnetic data by this method, it is indispensable to select samples suitable for measurement and to adopt an experimental protocol suited to the magnetic characteristics of the sample.

In this study we aim to categorize the magnetic carrier of plagioclase grains from gabbros to set a selection guideline of samples suitable for paleointensity measurements and optimize the Tsunakawa-Shaw paleointensity protocol to measure anisotropic samples. Gabbro samples collected at several localities in Tanzawa, Japan and Pilbara, Australia are studied. We measured the intensity of natural remanent magnetization (NRM) of ˜100 grains per gabbro sample and found that some samples showed NRM intensity distributing with large variability over several orders of magnitude while others had much smaller distribution. Optical microscope observation of selected specimens revealed that the former ones contain large opaque minerals while the later ones were dominated by tiny grains evenly distributed in some region of the plagioclase grain. These results can be interpreted that random capturing of magnetic inclusions with various size and origin during crystal growth of plagioclase can result in large variability in NRM intensity, and without such inclusions exsolved magnetite whose concentration and size distribution controlled by the chemical and thermal condition at the locality can be the main source of magnetization. Therefore, the distribution of NRM intensity can be useful to select magnetically stable samples with exsolved magnetite.

Large magnetic anisotropy biases the results of paleomagnetic measurements by (i) tilting the direction of the remanent magnetization from that of external field toward that parallel to the easy axis, and (ii) varying efficiency of remanent magnetization acquisition by the direction relative to the anisotropy axes. Therefore, we propose to add the following procedures to the Tsunakawa-Shaw protocol in the paleointensity measurement of single plagioclase grains: After stepwise demagnetization of NRM, impart anhysteretic remanent magnetization (ARM) to three orthogonal directions to approximate the degree of anisotropy and estimate the number of specimens required to cancel the anisotropy bias. For samples with large anisotropy for which an unrealistic number of specimens are required, measure ARMs imparted to 6 more orientations to determine the anisotropy tensor precisely. From this tensor and the direction of NRM, calculate the direction of the paleomagnetic field in the sample coordinate system. Impart ARM0 in a DC field parallel to the calculated paleomagnetic field direction to minimize the bias on paleointensity caused by anisotropy. In the presentation, we will discuss the guidelines for applying the above protocol based on the results of anisotropy measurements of some samples.

R004-12
Zoom meeting A ：11/4 PM1 (13:45-15:30)
14:00〜14:15

Paleomagnetic directions and intensities from volcanic rocks in the Tendaho Graben in the Afar depression, Ethiopia

#Haotian Liu[1)],Nobutatsu Mochizuki[2)],Chie Kato[3)],Tesfaye Kidane[4)],Ameha Muluneh[5)],Masakazu Fujii[6)],Ryokei Yoshimura[7)], Shin-ichi Kagashima[8)],Yo-ichiro Otofuji[9)],Naoto Ishikawa[10)]
([1]Kumamoto Univ.,[2]Kumamoto University,[3]Division of Earth Sciences, SCS, Kyushu Univ.,[4]University of KwaZulu Natal, South Africa,[5]Addis Ababa Univ.,[6]NIPR,[7]DPRI, Kyoto Univ.,[8]Yamagata Univ.,[9]Japan Geochronology Network, Japan,[10]School of Sustainable Design, The University of Toyama

The Afar depression is one of the unique areas for the study of the spreading centers. Magnetic anomaly observation and paleomagnetic measurements in Afar area are considered to be important to understand the magnetization structure of the spreading axis. In this study, paleomagnetic measurements were made on the samples from volcanic rocks of 43 sites across the spreading axis in the Tendaho Graben in Afar.For specimens of the 43 sites, 16 specimens were measured by thermal demagnetization and 84 specimens were measured by alternating field demagnetization. Checking remanent magnetization directions for each site shows that four sites directions are less reliable. We adopt the other 83results from 39 sites which give reliable paleomagnetic directions, and calculate the mean-site directions. Combining our data with the reported data of 21 sites, paleomagnetic directions are obtained for 60 sites across the spreading axis in the Tendaho Graben. For the 60 sites, 41 sites show normal polarity, 17 sites have reverse polarity, and 2 sites show intermediate directions. The paleomagnetic polarity shows a simple pattern along the line vertical to the spreading axis, which is reverse-normal-reverse polarity from southwest to northeast. The normal polarity zone is observed at the spreading axis with a width of about 40 km and the reverse polarity zones are recognized at both sides of the normal zone. We have also conducted paleomagnetic intensity measurements by the Tsunakawa-Shaw method. Up to now, preliminary paleointensity results were obtained from a specimen for each of 28 sites. Seventeen out of the 28 results passed the selection criteria. The obtained paleointensities range from 10 μ T to 42 μ T. The paleomagnetic direction and intensity data can give us a more precise time constraint on the formation process of the fissure lavas.

R004-13
Zoom meeting A ：11/4 PM1 (13:45-15:30)
14:15〜14:30

Analysis of magnetic mineral composition of a central North Pacific sediment core and its implications to RPI estimations

#Jiaxi Li[1)],Toshitsugu Yamazaki[1)]
([1]Atmosphere and Ocean Research Institute, The University of Tokyo

Abstract: Marine sediments contain considerable amounts and different types of magnetic mineral particles. Magnetic minerals in sediments may be statistically aligned to the direction of the ambient geomagnetic field so that sediments potentially preserve geomagnetic intensity records in the past. However, different types of magnetic minerals should preserve the remanent magnetization in different manners. And the compositional variation of magnetic mineral assemblages in marine sediments may hinder us from extracting reliable geomagnetic paleointensity records. The purpose of our research is to achieve more reliable relative paleointensity (RPI) estimations by understanding lithological contamination caused by compositional variations in marine sediments. We have made some progress regarding to this problem. Our research indicated that biogenic magnetite may possess lower RPI recording efficiency than terrigenous components in sediments taken from the Ontong-Java Plateau (OJP) in the western equatorial Pacific (Li et al., 2021, JpGU meeting). This is rather an unexpected result, contradictory to some previous studies (Ouyang et al., 2014; Chen et al., 2017). In order to achieve a more comprehensive understanding of the influence of compositional variations in sediments to RPI estimation, a sediment core taken from the central North Pacific (Core KR0310-PC1) was studied. Sedimentary environments in the central North Pacific are different from those in the western equatorial Pacific, which receive larger eolian dust inputs. The terrigenous component ought to be dominant in the central North Pacific sediments. Behaviors of different magnetic components to RPI recording can be expected to be deduced from sediments with a distinct lithological composition. RPIs were obtained by normalizing natural remanent magnetization (NRM) with both isothermal remanent magnetization (IRM) and anhysteretic remanent magnetization (ARM). The ratio of ARM susceptibility (k_{ARM}) to saturation isothermal remanent magnetization (SIRM) (k_{ARM}/SIRM) shows a downcore increasing trend which indicates an increasing proportion of biogenic to terrigenous magnetic minerals in the studied sediments. Estimations of relative proportion between biogenic and terrigenous components based on first-order reversal curve (FORC) diagrams are consistent with the increasing trend in the k_{ARM}/SIRM ratio. The results from FORC diagrams also indicate that the RPI records of high coercivity intervals are carried more by biogenic magnetites while the RPI records of low coercivity intervals are carried more by terrigenous magnetic minerals. On the other hand, NRM-IRM demagnetization diagrams show curvature, which indicates that the coercivity distributions of NRM and IRM are different. RPI recording efficiencies of different components were then assessed by recalculating the slopes in NRM-IRM demagnetization diagrams in corresponding coercivity intervals. The result indicates that biogenic magnetite possesses a higher RPI recording efficiency than the terrigenous components. This is the opposite of our previous conclusion from the western equatorial Pacific sediments. We speculate that different concentrations of silicate-hosted magnetic inclusions due to different sedimentary environments may be a possible reason for the contradiction. The contribution of the inclusions to NRM is minor in the western equatorial Pacific sediments (Li et al., 2021, JpGU meeting), while that in the central North Pacific sediments may be significant. Further studies on silicate-hosted magnetic inclusions with the help of chemical extraction experiment should help us to better understand its behavior in recording remanent magnetization in sediments.

Keywords: geomagnetic paleointensity, silicate-hosted magnetic mineral inclusion, biogenic magnetite, central North Pacific

R004-14
Zoom meeting A ：11/4 PM1 (13:45-15:30)
14:30〜14:45

南太平洋で採取されたマンガンノジュールの古地磁気学的解析による回転の復元

#片野田 航[1)], 小田 啓邦[2)], 村山 雅史[3)], 臼井 朗[4)]
([1] 高知大,[2] 産総研・地質情報,[3] 高知大学,[4] 高知大

Reconstruction of rotation by paleomagnetic analysis of manganese nodules collected in the South Pacific

#Wataru Katanoda[1)],Hirokuni Oda[2)],Masafumi Murayama[3)],Akira Usui[4)]
([1]Kochi University,[2]IGG, GSJ, AIST,[3]Kochi University,[4]Kochi Univ.

Marine manganese nodules are considered to grow at or within the deep-sea sediments, and assumed to have been uplifted and/or overturned during the growth without burial. We try to reconstruct the rotation and overturn during the growth process based on a paleomagnetic perspective using the manganese nodules collected with deep sea clay sediments. The Earth's magnetic field averaged over thousands of years can be approximated by a geocentric axial dipole, and the remanent magnetization direction recorded on the surface of a manganese nodule growing in a magnetic field is expected to correspond to the magnetic field direction at that time. If the manganese nodule has not rotated during the growth process, the paleolatitude can be determined by inclination of the remanent magnetization direction. On the other hand, if the manganese nodule has rotated, the paleolatitude calculated from inclination will be different from the actual latitude, and the amount of rotation can be detected from this discrepancy.

The nodules were collected by a box corer from the Penrhyn Basin (158-30-64W, 12-00-03S) at a water depth of 5248 m in the GH83-3 Hakurei-maru cruise conducted by the Geological Survey in 1983. A spherical sample (B92-1-1; 74 mm long, 60 mm wide, and 66 mm high) was chosen for the paleomagnetic analyses. The nodule was marked a dot on the apex (the center seen from directly above) with a white marker on board as a reference for the vertical direction.

The sample was split in half lengthwise along a plane including the white dot and the center of the nodule, and sample A was taken from the section as an upper half of a vertical slice of ˜10 mm thickness. Subsequently, another section was split in half along a plane, which is perpendicular to the first splitting plane, and sample B was taken similarly. Both slices were divided into five rows of strips, and then further divided into five subsamples by cutting perpendicular to the growth direction. Some samples were further divided into two perpendicular to the growth direction to allow detection of higher resolution changes in paleomagnetic and rock magnetic parameters with growth. The natural remanent magnetization of the subsamples was measured using a superconducting rock magnetometer (2G Enterprises Model 760R) at the National Institute of Advanced Industrial Science and Technology (AIST), and the stable remanent magnetization component was determined by stepwise AF demagnetization experiments. Furthermore, rock magnetic properties such as magnetic hysteresis, isothermal remanent magnetization acquisition curve, and First Order Reversal Curve (FORC) were measured using a vibrating sample magnetometer (Lakeshore VSM 8604). Magnetic property measurement was also carried out using the Magnetic Property Measurement System (MPMS: Quantum Design Inc.).

The paleomagnetic data confirmed that the paleomagnetic inclination of the samples near the surface around the white marker for both samples A and B are in good agreement with the inclination value (-23 degrees) expected for a geocentric axial dipole at the sampling locality. This confirms that the surface layer of the sample records the current geomagnetic field. In addition, paleomagnetic declination was corrected to zero and virtual geomagnetic poles (VGPs) were calculated. The VGPs continuously shifted to a position around equator 90 degrees to the northeast for a sample at 20 mm depth, suggesting that the Mn nodule may have rotated by about 90 degrees during the growth process. In addition, the results of zero-field-cycling of low-temperature magnetic measurements showed Verwey transition suggesting that the Mn nodule contain magnetite. The oldest sample (20 mm depth) did not show Verwey transition, which indicate that it was almost fully oxidized to maghemite. We discuss the possibility of rotation of manganese nodule during growth based on paleomagnetic directions, and the types and the origins of magnetic minerals based on rock magnetic data.

【はじめに】マンガンノジュール（以下, Mn nodule）は, Mn, Fe 酸化物のほかに Cu, Ni, Co, 希土類元素 (REE) などの有用金属元素を含有するため，将来の金属鉱物資源として開発が期待されている. また, 長期間の海洋環境を記録している堆積岩としても注目されている. これまでの研究と海底堆積物の表層から産出することなどにより，堆積物中に長時間埋没することなく成長し続けると考えられている.

【目的】Mn nodule の成長過程は十分に解明されておらず, 特に, 成長中に物理的な移動や回転などの運動があったのかは具体的に検証されていない. 本研究の目的は, 古地磁気学的解析から, Mn nodule の成長過程における回転運動の復元を試みて, 深海における堆積作用との関係を明らかにすることである. 数千年間の地球磁場を平均すると地心軸双極子で近似でき, 地球磁場中で成長する Mn nodule 表面に記録される残留磁化方位は, 当時の地球磁場方位に一致す

ることが期待される. Mn nodule が成長過程で回転していなければ, 残留磁化方位から当時の磁気伏角を求めることにより, 古緯度を求める事が可能である. 逆に, Mn nodule が回転していたとすれば, 磁気伏角から計算される古緯度は実際の緯度と異なる事になり, この食い違いから回転量の検出も可能である.

【試料】工業技術院地質調査所 (現, 産総研) によって 1983 年にペンリン海盆で実施された GH83-3 航海において, ボックスコアラーを用いて, 西経 158 度 30 分 64 秒, 南緯 12 度 00 分 03 秒, 水深 5248 m の深海粘土堆積物の表面から原位置のまま採取された, ほぼ球形 (B92-1-1; 74 mm x 60 mm x 66 mm) の試料を用いた. 採取時に試料の頂点 (中心) に, ホワイトマーカーで印をして鉛直上方向の基準とした. ダイヤモンドカッターを用いて, マーカーと Mn nodule の中心を含む面で垂直に半割して半割面から板状の A 試料を採取した. また, 残りの半割試料のマーカーを含む面で直交方向に分割して, その切断面から A 試料と直交する板状の B 試料を得た. A 試料, B 試料それぞれについて, 成長縞とほぼ直交するように縦方向に分割して 5 列の短冊状試料を切り出し, さらに成長縞とほぼ平行に 5 試料 (3.0 mm x 6.0 mm x 8.0 mm) あるいは 10 試料 (1.6 mm x 4.8 mm x 9.0mm) の小片に分割した.

【分析方法】成長に伴う古地磁気・岩石磁気パラメータの変化を測定した. 試料の自然残留磁化は, 産業技術総合研究所のパススルー型超伝導岩石磁力計 (2G Enterprises Model 760R) を用いて測定し, 段階交流消磁実験と消磁曲線の解析により初生残留磁化成分を求めた. また, 超伝導岩石磁力計を用いて非履歴性残留磁化の測定も行った. さらに, 振動試料型磁力計 (Lakeshore 社 VSM 8604 型) を用いて, 磁気ヒステリシス, 等温残留磁化獲得曲線, FORC（First Order Reversal Curve）などの岩石磁気特性を測定し, Magnetic Property Measurement System(MPMS:カンタムデザイン社) を用いて低温磁気測定を行った.

【結果】A 試料, B 試料ともに、段階交流消磁の結果 12.5mT～80mT の範囲で原点に向かう初生と思われる安定磁化成分を確認することができた。これら安定磁化成分から計算した磁化方位から、ホワイトマーカー近くの表面付近の試料の古地磁気伏角は試料採取地点で期待される地磁気伏角（-23 度）とよく一致することが確認された. このことから, ノジュールの表層は, 現在の地磁気を記録していることが確認できた. また、表面試料の古地磁気偏角がゼロになるように補正して、見かけの古地磁気極（VGP）を計算した。この結果によると、VGP は北極近く（表面試料）から北東方向に約 90 度離れた赤道付近（深さ 20 mm の試料）に向かって連続的に変化することが確認された。従って, Mn nodule は成長過程において約 90 度回転したと推定される. また, 低温磁気測定の Zero-Field-cycling の結果で Verwey 転移が確認できることなどから, Mn nodule は磁鉄鉱を含むと推定される。しかし、最も古い深さ 20 mm の試料では Verwey 転移が確認できず、ほぼ完全に酸化したマグヘマイトを多く含むと考えられる. 本発表では、古地磁気方位の結果に基づいて Mn nodule の成長中の回転の可能性について論じるとともに, 岩石磁気データに基づく磁性鉱物の種類と起源についても考察する.

R004-15
Zoom meeting A ：11/4 PM1 (13:45-15:30)
14:45〜15:00

ラハール堆積物の定置年代と定置温度の推定とナノバブルを用いた還元化学消磁

#池田 暁 [1)], 中村 教博 [1,2)], 佐藤 哲郎 [3)]
[(1] 東北大学理学研究科地学専攻,[(2] 東北大学高度教養教育・学生支援機構,[(3] 東京大学地震研究所

Reductive chemical demagnetization with ultrafine bubbles technology for estimation of Lahar‘s emplaced age and temperature

#akira ikeda[1)],norihiro nakamura[1,2)],tetsuro sato[3)]
[(1]Department of Earth Science, Tohoku University,[(2]Institute for Excellence in Higher Education, Tohoku University,
[(3]Earthquake Research Institute, The University of Tokyo

Lahars are extremely destructive debris flow of mud-rock slurries, sometimes including boulders. In lahars, the presence of such boulders has well been known worldwide. The application of VRM dating to lahar boulders possesses the potential for reconstructing the occurrence of lahar events. We now focus on the andesite boulders in Sukawa lahars at the western foot of Adatara volcano, Northeast Japan. The paleomagnetic measurement of lahar boulders also allows us to estimate the lahar‘s emplaced temperature. However, some boulders have hydrothermally been altered in-situ or nearby the crater at the Adatara summit, representing the different direction of characteristic remanence. Moreover, the precipitation of hydrothermally iron-oxides would also lead us to mislead unblocking temperatures of VRM components during thermal demagnetizations. Therefore, we apply new reductive chemical demagnetization (RCD) by Anai et al. (2018) to dissolve ferric iron (Fe^{3+}) in secondary goethite and pigment hematite precipitated in voids and or cracks in samples, with ultrafine bubbles technology to our samples for chemical demagnetization. In this presentation, we will show MPMS, paleomagnetic conglomerate test and paleomagnetic VRM dating.

ラハールは火山地域で発生する流動現象の一種で, 山麓において壊滅的な被害を引き起こす. ラハール堆積物中の古木の放射性炭素年代と層位学から, その地域の災害史を復元する研究が行われているが, いつでも古木が含まれるわけではない. 一方, ラハール堆積物にはしばしば火口付近や斜面に定置していた巨礫が含まれることがある. 近年, 巨礫に対して粘性残留磁化を用いて年代を推定する方法が考えられている (Sato et al., 2014, 2016, 2019). 本調査地域である安達太良火山西麓酸川流域に広がるラハール堆積物中は, 安山岩起源の巨礫が多数含まれているものの, 個々の巨礫は熱水変質を被っており, ２次的な鉄酸化物が岩石表面や割れ目にそって抄出している. そのため, コア試料を段階熱消磁すると, 現在の地球磁場とは異なる初生磁気を示していた. そこで, 本研究では Anai et al. (2018) で提案された還元化学消磁 (RCD) という新しい手法を用いて, 二次磁性鉱物中の Fe^{3+} をアスコルビン酸により還元・溶解させることで取り除くことを試みた. このときコア試料を, 超微細泡 (ナノバブル) を発生させる装置にアスコルビン酸溶液とともに浸し, 溶液を循環させた. この還元化学消磁による前処理を実施した結果, 現在の地球磁場に近い初生磁気を取り出すことができた. また, 処理前の低温 SQUID 磁気測定の結果, 250K への冷却時に室温 IRM がごく僅かに上昇するために, 針鉄鉱の存在が示唆され, また高磁場での冷却加熱実験における 50K 付近の急減により, ナノサイズの磁鉄鉱もしくは磁硫鉄鉱の存在が示唆される. また, 明瞭な Verway 点が見られないことから, 磁鉄鉱が酸化された赤磁鉄鉱の可能性もある. これらのうち, 針鉄鉱が還元化学消磁されたものと考えられる. 本発表では, これらの低温磁気測定の結果に加えて, 野外礫岩テストの結果も加えて, ラハール中の巨礫の定置年代と定置温度の測定結果を報告する.

R004-16
Zoom meeting A ：11/4 PM1 (13:45-15:30)
15:00〜15:15

堆積物形成初期に磁性細菌 Magnetospirillum magnetotacticum MS-1 が獲得する残留磁化の検討－細胞の配向を抑制した系

#政岡 浩平 [1)], 諸野 祐樹 [2)], 山本 裕二 [3)], 大野 正夫 [1)]
([1] 九州大学,[2] 海洋研究開発機構　高知コア研究所,[3] 高知大学

The properties of remanent magnetization carried by magnetotactic bacteria - system with suppressed cells orientation

#Kohei Masaoka[1)],Yuki Morono[2)],Yuhji Yamamoto[3)],Masao Ohno[1)]
([1]Kyushu University,[2]Kochi Institute for Core Sample Research, Japan Agency for Marine-Earth Science and Technology, [3]Kochi University

Variation of the past geomagnetic field is recorded in marine sediments as a fossil magnetization, called natural remanent magnetization (NRM). NRM is carried not only by detrital magnetic grains but also by biogenic magnetic grains originated from magnetotactic bacteria. To investigate characters of NRM carried by biogenic magnetic grains we have cultured the magnetotactic bacteria Magnetospirillum magnetotacticum MS-1 (here under, MS-1) in the laboratory and made samples using them for remanent magnetization measurements by simulating a very early process of sediment formation. The samples were made at the different start times of the magnetic field applied to examine the effect of viscosity. We will report and discuss the results.

海底堆積物には自然残留磁化（NRM）として，過去の地磁気の変動がほぼ連続的に記録されている．この NRM は陸源などの無機的に形成された磁性鉱物だけでなく，磁性細菌に由来する生物源の磁性細菌にも担われている．NRM の 20-30 パーセントが生物源マグネタイトによって担われると推定される堆積物もあり，その量的な重要性が指摘されている（e.g. Yamazaki, 2012; Yamazaki and Ikehara, 2012). しかし，堆積物が獲得する NRM の性質について，培養系の磁性細菌を起源とする生物源マグネタイトを用いて実験室環境下でその獲得プロセスを模擬し，検討している例は Paterson et al. (2013) に限られる．我々は，培養した磁性細菌 Magnetospirillum magnetotacticum MS-1(以下 MS-1) の細胞群を用いて，地球磁場を模した外部磁場を含む様々な条件下で「堆積物形成初期」の過程を模擬した実験を行って試料群を作製し，それらの磁気的性質の系統的検討を進めている (政岡ほか, 2018JpGU, 2018SGEPSS, 2019JpGU, 2019SGEPSS, 2020JpGU, 2021JpGU). 試料群の作製は，50 度で恒温保持した状態で，融解させた寒天に MS-1 の細胞群を混合し，その後，外部磁場下で室温まで冷却して寒天を固結させることで行っている．これまでに，NRM 強度が印加磁場強度の増加に対して非直線的に増加することや，NRM/ARM 比や NRM/IRM 比が実際の堆積物から報告される値よりも 1 桁以上大きいことなどを報告した.

今回は，MS-1 の細胞群の外部磁場方向への配向効率を変化させた試料群を作製して磁気的性質を検討することを目的として，50 度からの冷却時に外部磁場を印加する時刻を変化させて試料群を作製した．寒天の粘性は温度の低下に伴って増加するため (加藤, 1960)，より低い温度で外部磁場を印加して作製した試料ほど，MS-1 の細胞群の配向は抑制されているはずである．試料群の作製にあたり，基本的手順は政岡ほか (2020JpGU) と同様とした．まず，融解させた寒天と MS-1 の細胞群を混合し 50 度で恒温保持した (3.0×10^9 cells/7 cc, 14 試料分)．そして，外部磁場印加用のヘルムホルツコイル内に静置した後，磁場印加開始時刻を，0-13 分の範囲で変化させて試料群を作製した．磁場印加開始時刻における試料の表面温度を，放射温度計で測定した．印加した磁場の強度は 50 μ T，方位は偏角 0 度・伏角 0 度で，試料群の座標系は，印加磁場と一致する方向に x 軸，偏角＋ 90 度・伏角 0 度の方向に y 軸，伏角＋ 90 度の方向に z 軸とした．これらにより獲得された残留磁化を NRM と見なして分析し，さらに，各試料の xyz 各軸方向に ARM を着磁して分析した．結果の概要は以下の通りである.

(1)NRM 方位は，時刻 0-10 分の試料群については印加磁場方位とよく一致した．時刻 11-13 分の試料群については，わずかに（偏角: ˜1.8 度，伏角: ˜0.6 度）異なる方位であった.

(2) NRM 強度は，磁場印加開始時刻 0-2 分 (表面温度˜40 度) の試料群は $1.50 \pm 0.062 \times 10^{-9}$ Am^2 とほぼ一定であるが，時刻 3-7 分の試料群から緩やかな減少傾向を示し始めた．時刻 8-10 分 (表面温度˜33 度) の試料群では時刻 0-2 分の試料群の 17 パーセントの強度まで急激に減少し，時刻 11-13 分の試料群では時刻 0-2 分の試料群の 8.5 パーセントの強度でほぼ一定となった．この NRM 強度は，MS-1 の細胞群を含有しないブランク試料の NRM 強度と同程度であった.

(3)ARM 強度は，時刻ゼロに近い試料群は大きい残留磁化異方性を示す一方（ARMy,z に対して ARMx は 1.8 倍程度大きい），時刻の増大に伴い異方性は減少し，時刻 11-13 分の試料群では異方性はほぼ見られなかった.

以上の結果から，磁場印加開始時刻が遅いほど，NRM 方位の一致度が悪くなり，NRM 強度も弱くなることと，ARM の残留磁化異方性が小さくなることがわかる．時刻が遅いほど試料表面温度が低く磁場印加開始時の寒天の粘性が増大しており，外部磁場に対する MS-1 の細胞群の配向が抑制されたと考えられる．温度条件などさらなる検討が必要であるが，寒天の粘性を増加させることで NRM/ARM 比を「低下」させた「堆積物形成初期」の模擬試料を作製することができ，実際の堆積物にみられる NRM/ARM 比に近い模擬試料の磁気的性質の検討に道を開く可能性がある.

R004-17
Zoom meeting A ：11/4 PM2 (15:45-18:15)
15:45〜16:00

Basic properties of shock remanent magnetization for single-domain titanomagnetite

#Masahiko Sato[1)],Kosuke Kurosawa[2)],Shota Kato[1)],Masashi Ushioda[3)],Sunao Hasegawa[4)],Futoshi Takahashi[5)]
([1]The University of Tokyo,([2]Chiba Institute of Technology,([3]Shikoku Research Institute Inc.,([4]Japan Aerospace Exploration Agency,([5]Kyushu University

Shock remanent magnetization (SRM) is acquired as a result of the shock wave propagation in a magnetic field. Knowledge of a three-dimensional distribution of the SRM intensity is crucial for interpreting the spatial change in magnetic anomalies observed over the crater and reconstructing the paleo-planetary field based on the anomaly data. However, the intensity distribution is an unexplained phenomena concerning SRM properties owing to the lack of subsample magnetization measurements for the experimental SRM-imparted samples. To investigate the SRM intensity and stability structures using a magnetically well-characterized basalt sample bearing fine-grained single-domain titanomagnetite, we conducted the newly designed SRM acquisition experiments and remanence measurements for cube-shaped subsamples cut from the SRM-imparted samples. The pressure and temperature changes during the shock wave propagation were estimated from the impact simulations. From the experimental results of cylindrical samples with 10 cm in diameter and length, three distinctive aspects of SRM properties are recognized at different pressure ranges: (1) the SRM intensity is almost constant below 0.1 GPa, (2) the SRM intensity linearly increases with increasing pressure up to 1.1 GPa, and (3) the SRM intensity is almost constant, while the SRM stability increases with increasing pressure above 1.9 GPa. Regarding the SRM acquisition mechanisms, the pressure effect was likely dominant below 1.1 GPa, while multiple factors can be considered in the high-pressure range. The systematic changes in the SRM intensity and stability suggest that the crustal rocks containing the single-domain titanomagnetite had an SRM intensity structure at the time of impact, and this structure changed subsequently. Comparing the SRM structures of different experimental settings such as target size, projectile condition, and field intensity, we will evaluate the basic properties of SRM and will discuss the remanence acquisition mechanisms.

R004-18
Zoom meeting A ：11/4 PM2 (15:45-18:15)
16:00〜16:15

Preliminary study of high resolution monitoring of paleomagnetic experiments with reef limestones

#Chisato Anai[1)],Hirokuni Oda[2)]
([1]Aso Volcanological Laboratory, Kyoto Univ.,[2]IGG, GSJ, AIST

Reef limestone has very week remanent magnetization. Previous studies (e.g. Anai et al., 2018) suggest that magnetite seems to be the main carrier of the weak magnetism, and other magnetic minerals crystallized secondarily (e.g. hematite and/or goethite) are also present. The origin of magnetite is considered to be biogenic and/or detrital, which is not clear at the moment. Reef limestones are composed of coral and other fossils with significant heterogeneity in the samples and their magnetizations are weak in general. For this reason, standard magnetization measurement using superconducting magnetometer is quite difficult for some samples. Against this background, reef limestone has been considered to be an unsuitable subject for paleomagnetic studies including magnetostratigraphy. On the other hand, reef limestone is known to be an excellent recorder of paleoenvironment, such as sea-level change and/or climate change. In order to retrieve high sensitivity paleomagnetic and rock magnetic information from reef limestones at sub-millimeter scales, we conducted analyses using a scanning SQUID microscope on a thin section.

Typical characteristic behavior of reef limestones during AF demagnetization is that they are unstable showing inconsistencies among multiple trials at each demagnetization step. We considered the possibility that this could be caused by unstable domain wall movements of MD particles. From the results of SQUID microscopy, the unstable (possible MD) particles seem to be attached to the cavities in the samples. This is consistent with previous studies in which secondary magnetic minerals were removed by flowing a reducing etchant through the cavities of the samples. The high porosity and extremely high permeability of reef limestone suggest that secondary magnetic minerals are crystallized and attached when water containing divalent iron ions passes through the pores. The possible MD particles, which could be responsible for the instability against demagnetization, are also likely to be secondary crystals. The results of an XRF scanner on the thin section also support this prediction. The XRF analysis show that the Fe component is concentrated on the fossil surface and on the walls of the cavities, indicating the presence of secondary magnetic minerals attached to the water channels in the reef limestones. Based on these results, we considered that removing iron oxides and/or iron hydroxides attached to the boundaries between particles and on the surfaces of the cavities can reduce instability against demagnetization and measurement noise. In order to clarify the hypothesis, we plan to conduct chemical demagnetization on a reef limestone sample while monitoring magnetization and chemical composition with the scanning SQUID microscope and the XRF scanner. In the presentation, we will further show experimental results and evaluate the hypothesis.

R004-19
Zoom meeting A ：11/4 PM2 (15:45-18:15)
16:15〜16:30

土器片に対する岩石磁気学 －「考古岩石磁気学」の確立に向けて－

#畠山 唯達 [1)], 八木 千亜希 [2)], 白石 純 [2)]
[(1] 岡山理大・フロンティア理工学研,[(2] 岡山理大・生物地球

Rock magnetism of old ceramics: way to establishment of archaeo-rock magnetism

#Tadahiro Hatakeyama[1)],Chiaki Yagi[2)],Jun Shiraishi[2)]
[(1]IFST, Okayama University of Science,[(2]Faculty of Biosphere-Geosphere Science, Okayama University of Science

In the ceramics such as the potteries excavated from ancient kilns, the minerals contained in the raw materials (clays) were dehydrated and transformed into other stable minerals in the high-temperature environment. The status of the baking, temperature, oxidation, are very complicated and widely variated even in a kiln, so that they create greater variation in colors, porosity and other characteristics of the ceramics. We focus on the iron-baring minerals, mainly iron oxides, in the ancient ceramics to estimate the characteristics of the kiln and manufacturing works of them. Here we report the magnetic properties, magnetic susceptibility, magnetic hysteresis parameters, IRM acquisition spectra, response to the magnet, compared with the iron content derived from X-ray fluorescence analyses. We will show the variation of the magnetic and chemical parameters samples from one kiln and estimate the characterization of the kiln from them.

窯で焼成された土器（陶器）では、素材となる粘土中に含まれる鉱物・化合物が火焔中で脱水・変質して高温で安定な鉱物となる。変質の過程は複雑で、地域や異なる窯間ではもちろん、同一窯内でも操業回や窯内位置によって焼成のされ方が異なることが多く、表面や内部の多彩な色、焼き締まり度合などに反映していると考えられる。土器に含まれる様々な鉱物のうち、温度や酸化状態を反映し、色に現れるものの代表として鉄鉱物が挙げられる。焼成後の鉄鉱物の多くは鉄酸化物で、鉄酸化物の多くは強磁性鉱物でもある。そこで本研究では、岩石磁気学的手法を発掘された土器片に対して適用し、土器・土器窯体に含まれる鉄鉱物の磁性とそのバリエーションを調べた。岡山県瀬戸内市の庄田工田 (くでん) 窯跡から出土した表面採取土器片約 100 点に対し、蛍光 X 線分析から得られた鉄の含有量と帯磁率、磁気履歴パラメータ、等温残留磁化獲得スペクトル、磁石を近づけた時の応答、などを比較し、一つの窯跡から入手できる試料内でどれくらいの岩石磁気的な分布を示すかを紹介する。

R004-20
Zoom meeting A ：11/4 PM2 (15:45-18:15)
16:30〜16:45

超伝導岩石磁力計のセンサー感度曲線：古地磁気個別試料の形状による誤差の評価

#小田 啓邦 [1)],Xuan Chuang[2)]
(1 産総研・地質情報,(2National Oceanography Centre Southampton

Sensor response of superconducting rock magnetometer: Evaluation of errors of discrete paleomagnetic samples with various shapes

#Hirokuni Oda[1)],Chuang Xuan[2)]
(1IGG, GSJ, AIST,(2National Oceanography Centre Southampton

Superconducting rock magnetometers (SRMs) are fundamental to paleomagnetism research as they enable rapid and precise measurement of remanence preserved in geological and archaeological archives. However, SRM measurements are smoothed and distorted due to convolution effect of the SRM's sensor response, and deconvolution is necessary to restore high resolution and more accurate remanence signal (see Oda and Xuan, 2014; Xuan and Oda, 2015; Oda et al., 2016). Successful deconvolution relies on accurate estimate of SRM's sensor response. We developed a software URESPONSE to facilitate accurate estimate of SRM sensor response based on repeated measurements of a magnetic point source (see Xuan and Oda, 2019). We demonstrate the difference in sensor response between an old liquid-helium-cooled SRM and a new liquid-helium-free SRM at the University of Southampton. We show that normalization of measurement data using a nine-element "effective-length" matrix calculated from sensor response estimate reduces differences in measurement data, and deconvolution using accurate sensor response estimates yields highly consistent and high-resolution results for data from the two SRMs.

In addition, we measured a thin section sample both on an SRM and on a scanning SQUID microscope (SSM) at the Geological Survey of Japan (Pastore et al., 2021). URESPONSE was used to calculate average magnetization and magnetic moment of the thin section for SRM measurements. We show that magnetic moment calculated using the SRM data is consistent with the sum of estimated magnetic moments of individual magnetic grains within the thin section (Pastore et al., 2021) only if accurate estimate of SRM sensor response (including all cross terms) are used. Development is ongoing to integrate SRM sensor response over the volume of a discrete sample with various shapes to restore accurate magnetic signal preserved in the samples. Evaluation will be done to see differences with corrections using sensor responses calculated for discrete sample volumes with various shapes.

References

Oda and Xuan (2014) Earth Planets Space, 67, 183.
Oda et al. (2016) Earth Planets Space, 68, 1-13.
Xuan and Oda (2015) Geochem. Geophys. Geosyst., 15, 3907-3924.
Xuan and Oda (2019) Geochem. Geophys. Geosyst., 20, 4676-4692.
Pastore et al. (2021) Geochem. Geophys. Geosyst., 22, e2020GC009580.